Proceedings of the
47th IEEE Conference on Decision and Control
Cancun, Mexico, Dec. 9-11, 2008

ThB09.6

Algorithm for Reducing the Number of Constraints of POD-based Predictive Controllers

Oscar Mauricio Agudelo, Jairo José Espinosa, *Senior Member, IEEE,*
and Bart De Moor, *Fellow Member, IEEE*

Abstract— This paper introduces an algorithm for reducing the number of temperature constraints of a POD-based predictive controller for a non-isothermal tubular reactor. Apart from keeping the process operating around some nominal conditions, the control system has to maintain the temperature inside the reactor below a certain limit in order to avoid undesirable side reactions. The controller uses a reduced order model of the process, which is derived by means of the Proper Orthogonal Decomposition (POD) and Galerkin projection techniques. The use of a reduced order model is necessary due to the high dimensionality of the discretized system used to approximate the Partial Differential Equations (PDEs) that model the reactor. Although a big order reduction can be obtained with the POD technique, this technique does not reduce the number of temperature constraints which is typically very large. The algorithm proposed in this paper reduces dramatically the number of temperature constraints, and consequently the memory needed for storing them and the time required for solving the optimization of the predictive controller.

I. INTRODUCTION

Proper Orthogonal Decomposition (POD) is a technique that has been applied in many physical systems modeled by Partial Differential Equations (PDEs) for deriving reduced order models, making possible the design and implementation of controllers for these systems. The advantage of applying POD is the incorporation of simulation or experimental data as well as the existing physical relationships from the original model [1].

In [2], a POD-based predictive controller is proposed for controlling the temperature and concentration profiles of a non-isothermal tubular chemical reactor. The control goal is to reject the disturbances that affect the process, that is, the changes in the temperature and concentration of the feed flow. One important constraint of the system is that the temperature inside the reactor must be below 400 K in order to prevent undesirable side reactions. Since this constraint is not incorporated in the formulation of the predictive controller, temporary violations of the temperature constraint

O. M. Agudelo is with the Department of Electrical Engineering (ESAT), Research Group SCD-SISTA, Katholieke Universiteit Leuven, Kasteelpark Arenberg 10, B-3001 Heverlee (Leuven), Belgium. He is also with the Department of Automation and Electronics, Universidad Autónoma de Occidente, Calle 25 No 115-85, Cali, Colombia. `mauricio.agudelo@esat.kuleuven.be`

J. J. Espinosa is with the Facultad de Minas, Universidad Nacional de Colombia, Carrera 80 No. 65-223, Medellin, Colombia. `jairo.espinosa@ieee.org`

B. De Moor is with the Department of Electrical Engineering (ESAT), Research Group SCD, Katholieke Universiteit Leuven, Kasteelpark Arenberg 10, B-3001 Heverlee (Leuven), Belgium. `bart.demoor@esat.kuleuven.be`

can be observed when large disturbances are applied. In [3], an extension of such control system is presented, which takes into account the temperature constraint of the reactor and uses a slack variable approach with ℓ_∞-norm and time-dependent weights for handling the infeasibilities that can emerge [4]. Although POD can find a reduced order model for the reactor, it does not reduce the number of temperature constraints, and therefore the controller has to deal with a very large number of them. In [3] a method for approximating the temperature constraints by means of the theory of positive polynomials is proposed. This approximation leads to a reduction in the number of constraints by replacing many inequalities by few Linear Matrix Inequalities (LMIs). In this approach the MPC optimization problem is written as a Semidefinite Program.

In this paper we propose an alternative way of reducing the number of temperature constraints which leads to a significant reduction of the memory requirements and computing time of the predictive controller. The method exploits the similarities between the coefficients of consecutive constraints and unlike other approaches, the MPC optimization problem is written as a Quadratic Program. This is the main contribution of this paper.

The paper is organized as follows. Section II presents a description of the tubular reactor. In Section III, the derivation of a reduced order model for the process using POD is discussed. Section IV shows a POD-based MPC control scheme that deals with a very large number of temperature constraints. In Section V, we present our algorithm for reducing the number of temperature constraints. Section VI shows some simulation results and finally Section VII draws the main conclusions.

II. TUBULAR REACTOR

The process to be controlled is a non-isothermal tubular reactor where a single, first order, irreversible, exothermic reaction takes place $(A \rightarrow B)$. The reactor is surrounded by 3 cooling/heating jackets as shown in Figure 1. The temperature of the jacket fluids $(T_{J1}, T_{J2}$ and $T_{J3})$ can be manipulated independently in order to control the concentration and temperature profiles in the reactor. If a plug-flow behavior is assumed in the system, the mathematical model of the reactor is given by the following non-linear PDEs:

$$\frac{\partial C}{\partial t} = -v\frac{\partial C}{\partial z} - k_0 C e^{-\frac{E}{RT}}$$

$$\frac{\partial T}{\partial t} = -v\frac{\partial T}{\partial z} + G_r C e^{-\frac{E}{RT}} + H_r(T_w - T) \quad (1)$$

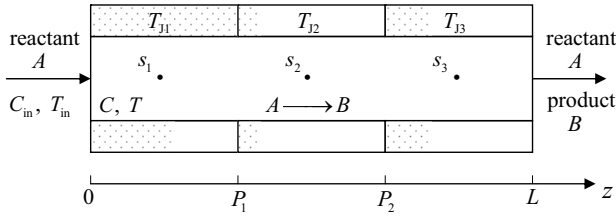Fig. 1.   Tubular Reactor with 3 cooling/heating jackets.

$$G_{\mathrm{r}} = \frac{-\Delta H k_0}{\rho C_{\mathrm{p}}}, \quad H_{\mathrm{r}} = \frac{4h}{2r\rho C_{\mathrm{p}}}$$

with the following boundary conditions:

$$C = C_{\mathrm{in}} \text{ at } z = 0 \text{ and } T = T_{\mathrm{in}} \text{ at } z = 0,$$

where $C(z,t)$ is the reactant concentration in [mol/L], $T(z,t)$ is the reactant temperature in [K], v is the fluid superficial velocity in [m/s], $(-\Delta H)$ is the heat of the reaction in [cal/mol], ρ and C_{p} are the density in [kg/L] and the specific heat in [cal/kg/K] of the mix respectively, k_0 is the kinetic constant in [1/s], E is the activation energy in [cal/mol], R is the ideal gas constant in [cal/mol/K], h is the heat transfer coefficient in [cal/s/m^2/K], r is the reactor radius in [m], L is the reactor length in [m], C_{in} and T_{in} are the concentration in [mol/L] and the temperature in [K] of the feed flow, z is the axial coordinate in [m], t is the time in [s] and $T_{\mathrm{w}}(z,t)$ is the reactor wall temperature in [K] defined as follows (see Figure 1): $T_{\mathrm{w}} = T_{\mathrm{J1}}$ for $0 \leq z < P_1$, $T_{\mathrm{w}} = T_{\mathrm{J2}}$ for $P_1 \leq z < P_2$ and $T_{\mathrm{w}} = T_{\mathrm{J3}}$ for $P_2 \leq z \leq L$.

The parameters of the reactor model are taken from [5], which were inspired by the values given in [6]. These values are: $v = 0.1$ m·s^{-1}, $L = 1$ m, $k_0 = 10^6 \cdot$s^{-1}, $E = 11250$ cal·mol^{-1}, $R = 1.986$ cal·mol^{-1}·K^{-1}, $C_{\mathrm{in}} = 0.02$ mol·L^{-1}, $T_{\mathrm{in}} = 340$ K, $G_{\mathrm{r}} = 4.25 \cdot 10^9$ L·K·mol^{-1}·s^{-1}, and $H_{\mathrm{r}} = 0.2$ s^{-1}.

The temperature of the jacket sections T_{J1}, T_{J2} and T_{J3} must be between 280 K and 400 K. In addition, the temperature inside the reactor must be below 400 K in order to avoid the formation of side products. The sort of disturbances that affects the reactor are mainly the variations in the temperature and concentration of the feed flow. Typically, such variations are in the range of ± 10 K for the temperature and $\pm 5\%$ of the nominal value for the concentration. In this system, only the temperature of the feed flow is measured directly. Additionally, the reactor has a temperature sensor at the output and 3 temperature sensors (s_1, s_2 and s_3) distributed in its interior as shown in Figure 1.

A. Operating Profiles

In [2], an optimization algorithm (a kind of SQP) is proposed for deriving the optimal operating profiles of the tubular reactor described by (1). The algorithm minimizes a given cost function subject to the steady-state equations of the reactor and the input and temperature constraints of the system. The operating profiles found in [2] are the profiles used in this paper, and they are shown in Figure 2 together with the jacket temperatures. Notice that the maximum
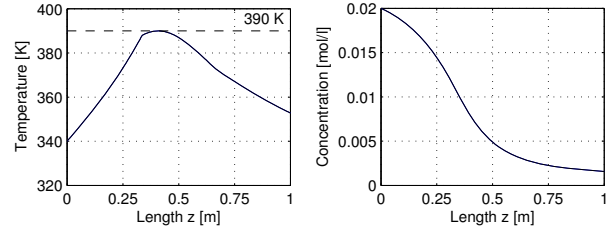
Fig. 2.   Steady-State profiles (operating profiles) when $T_{\mathrm{J1}} = 374.6$ K, $T_{\mathrm{J2}} = 310.1$ K and $T_{\mathrm{J3}} = 325.2$ K.

temperature along the reactor is 390 K. In the steady-state optimization algorithm, the maximum temperature allowed inside the reactor was set 10 degrees below the actual limit (400 K) in order to give to the predictive controller enough room of maneuverability.

B. Linear Model

As it was done in [2], the linear model of the tubular reactor is obtained by linearizing (1) around the jacket temperatures and the operating profiles presented in Figure 2. Subsequently, the infinite dimensionality of the resulting linear PDEs is reduced by replacing the partial derivatives with respect to space by backward finite difference approximations, giving as result the following system of Ordinary Differential Equations (ODEs):

$$\dot{\mathbf{x}}(t) = \mathbf{A}\mathbf{x}(t) + \mathbf{B}\mathbf{u}(t) + \mathbf{F}\mathbf{d}(t) \qquad (2)$$

$$\mathbf{x}(t) = (\bar{C}_1^{\Delta}, \bar{C}_2^{\Delta}, ..., \bar{C}_N^{\Delta}, \bar{T}_1^{\Delta}, \bar{T}_2^{\Delta}, ..., \bar{T}_N^{\Delta})^T$$

$$\mathbf{d}(t) = (\bar{C}_{\mathrm{in}}^{\Delta}, \bar{T}_{\mathrm{in}}^{\Delta})^T, \quad \mathbf{u}(t) = (\bar{T}_{\mathrm{J1}}^{\Delta}, \bar{T}_{\mathrm{J2}}^{\Delta}, \bar{T}_{\mathrm{J3}}^{\Delta})^T$$

where C_i^*, T_i^* are the steady state concentration and temperature of the ith section, C_{in}^* and T_{in}^*, are the steady state concentration and temperature of the feed flow, T_{J1}^*, T_{J2}^*, T_{J3}^* are the steady state jacket temperatures, T_{f} and C_{f} are normalization factors, $\bar{C}_i^{\Delta} = (C_i - C_i^*)/C_{\mathrm{f}}$, $\bar{T}_i^{\Delta} = (T_i - T_i^*)/T_{\mathrm{f}}$ are the normalized deviations from steady state of the concentration and temperature of the ith section, $\bar{C}_{\mathrm{in}}^{\Delta} = (C_{\mathrm{in}} - C_{\mathrm{in}}^*)/C_{\mathrm{f}}$ and $\bar{T}_{\mathrm{in}}^{\Delta} = (T_{\mathrm{in}} - T_{\mathrm{in}}^*)/T_{\mathrm{f}}$ are the normalized deviations from steady state of the concentration and temperature of the feed flow, $\bar{T}_{\mathrm{J1}}^{\Delta} = (T_{\mathrm{J1}} - T_{\mathrm{J1}}^*)/T_{\mathrm{f}}$, $\bar{T}_{\mathrm{J2}}^{\Delta} = (T_{\mathrm{J2}} - T_{\mathrm{J2}}^*)/T_{\mathrm{f}}$ and $\bar{T}_{\mathrm{J3}}^{\Delta} = (T_{\mathrm{J3}} - T_{\mathrm{J3}}^*)/T_{\mathrm{f}}$ are the normalized deviations of the jacket temperatures, N is the number of sections in which the reactor is divided, $\mathbf{A}$, $\mathbf{B}$ and $\mathbf{F}$ are the matrices describing the system, $\mathbf{x}(t)$ is the state vector, $\mathbf{u}(t)$ is the vector of the inputs, and $\mathbf{d}(t)$ is the vector of the disturbances.

Since the spatial domain of the reactor is divided into $N = 300$ sections, the number of states of (2) is equal to 600. This large number of states makes the design and implementation of feedback controllers for the reactor difficult. Hence it is necessary to find a reduced order model. In this study such a reduced order model is found using Proper Orthogonal Decomposition (POD) and Galerkin projection [7]. A detailed explanation of the procedure is given in [2]. However, in order to make this paper self contained, this procedure is presented briefly in the following section.

III. MODEL REDUCTION USING POD

In proper orthogonal decomposition (POD), we start by observing that $\mathbf{x}(t) \in \Re^{2N}$ can be expanded as a sum of orthonormal basis vectors:

$$\mathbf{x}(t) = \sum_{j=1}^{2N} a_j(t)\boldsymbol{\varphi}_j \qquad (3)$$

where $\boldsymbol{\varphi}_j \in \Re^{2N} \ \forall j = 1, \ldots, 2N$ is a set of orthonormal basis vectors (POD basis vectors or POD basis functions) in the discretized spatial domain, and $a_j(t) \in \Re \ \forall j = 1, \ldots, 2N$ are the time-varying coefficients, or POD coefficients, associated to each basis vector. These POD basis vectors are ordered according to their relevance to $\mathbf{x}(t)$.

The main dynamics of the system can be represented using the first n most relevant basis vectors, since $\boldsymbol{\varphi}_1, \boldsymbol{\varphi}_2, \ldots, \boldsymbol{\varphi}_n$ condensates the main spatial correlations. An nth order approximation of (3) is then given by means of the truncated sequence

$$\mathbf{x}_n(t) = \sum_{j=1}^{n} a_j(t)\boldsymbol{\varphi}_j, \ \ n \ll 2N. \qquad (4)$$

An approximate (reduced order) model of $\mathbf{x}(t)$ can be derived by building a model for the first n POD coefficients. This is the essence of model reduction by POD.

The POD basis vectors are determined from simulation or experimental data of the process. The dynamic model for the first n POD coefficients can be found by means of Galerkin projection [7]. In the following subsections, we describe the steps followed for deriving the reduced order model of (2).

A. Generation of the snapshot Matrix

We have constructed the snapshot matrix $\mathbf{X}_{\text{snap}} \in \Re^{600 \times 1500}$ from the system response when independent step changes were made in the input $\mathbf{u}(t)$ and perturbation $\mathbf{d}(t)$ signals of the linear model (2).

$$\mathbf{X}_{\text{snap}} = (\mathbf{x}(t = \Delta t), \ \ldots, \mathbf{x}(t = 1500\Delta t))$$

Along the simulations, 1500 samples were collected using a sampling time (Δt) of 0.05 s.

B. Derivation of the POD basis Vectors

The POD basis vectors were derived by calculating the singular value decomposition (SVD) of $\mathbf{X}_{\text{snap}}$,

$$\mathbf{X}_{\text{snap}} = \boldsymbol{\Phi}\boldsymbol{\Sigma}\boldsymbol{\Psi}^T$$

where $\boldsymbol{\Phi} \in \Re^{600 \times 600}$ and $\boldsymbol{\Psi} \in \Re^{1500 \times 1500}$ are unitary matrices, and $\boldsymbol{\Sigma} \in \Re^{600 \times 1500}$ is a matrix that contains the singular values of $\mathbf{X}_{\text{snap}}$ in a decreasing order on its main diagonal. The columns of $\boldsymbol{\Phi}$ are the POD basis vectors.

$$\boldsymbol{\Phi} \in \Re^{600 \times 600} = (\boldsymbol{\varphi}_1, \boldsymbol{\varphi}_2, \ldots, \boldsymbol{\varphi}_{600})$$

C. Selection of the most relevant POD basis vectors

We have made the selection by checking the singular values of $\mathbf{X}_{\text{snap}}$, the larger the singular value the more relevant the basis vector is. In this problem, the first 20 basis

vectors were selected. The 20th order approximation of $\mathbf{x}(t)$ is given by

$$\mathbf{x}_{20}(t) = \sum_{j=1}^{20} a_j(t)\boldsymbol{\varphi}_j = \boldsymbol{\Phi}_{20}\mathbf{a}(t), \qquad (5)$$

where $\boldsymbol{\Phi}_{20} = (\boldsymbol{\varphi}_1, \ldots \boldsymbol{\varphi}_{20})$ and $\mathbf{a}(t) = (a_1(t), \ldots, a_{20}(t))^T$.

D. Construction of the model for the POD coefficients

In order to derive a dynamic model for the POD coefficients, we have used the Galerkin projection. If we define a residual function $R(\mathbf{x}, \dot{\mathbf{x}})$ for equation (2) as follows:

$$R(\mathbf{x}, \dot{\mathbf{x}}) = \dot{\mathbf{x}}(t) - \mathbf{A}\mathbf{x}(t) - \mathbf{B}\mathbf{u}(t) - \mathbf{F}\mathbf{d}(t) \qquad (6)$$

and we replace $\mathbf{x}(t)$ by its nth order approximation $\mathbf{x}_n(t)$ in (6), the projection of $R(\mathbf{x_n}, \dot{\mathbf{x}_n})$ on the space spanned by the basis vectors $\boldsymbol{\Phi}_n$ shall vanish. That is,

$$\langle R(\mathbf{x}_n, \dot{\mathbf{x}}_n), \boldsymbol{\varphi}_j \rangle = 0; \ \ j = 1, \ldots, n \qquad (7)$$

where $\langle . , . \rangle$ denotes the Euclidean inner product. Replacing $\mathbf{x}(t)$ by its nth order approximation $\mathbf{x}_n(t) = \boldsymbol{\Phi}_n\mathbf{a}(t)$ in equation (2), and applying the inner product criterion (7) to the resulting equation we have:

$$\boldsymbol{\Phi}_n^T\boldsymbol{\Phi}_n\dot{\mathbf{a}}(t) = \boldsymbol{\Phi}_n^T\mathbf{A}\boldsymbol{\Phi}_n\mathbf{a}(t) + \boldsymbol{\Phi}_n^T\mathbf{B}\mathbf{u}(t) + \boldsymbol{\Phi}_n^T\mathbf{F}\mathbf{d}(t)$$

$$\dot{\mathbf{a}}(t) = \boldsymbol{\Phi}_n^T\mathbf{A}\boldsymbol{\Phi}_n\mathbf{a}(t) + \boldsymbol{\Phi}_n^T\mathbf{B}\mathbf{u}(t) + \boldsymbol{\Phi}_n^T\mathbf{F}\mathbf{d}(t).$$

The reduced order model of the reactor is then given by

$$\dot{\mathbf{a}}(t) = \mathbf{A}_r\mathbf{a}(t) + \mathbf{B}_r\mathbf{u}(t) + \mathbf{F}_r\mathbf{d}(t) \qquad (8)$$

$$\mathbf{x}_n(t) = \boldsymbol{\Phi}_n\mathbf{a}(t)$$

where $\mathbf{A}_r = \boldsymbol{\Phi}_n^T\mathbf{A}\boldsymbol{\Phi}_n$, $\mathbf{B}_r = \boldsymbol{\Phi}_n^T\mathbf{B}$ and $\mathbf{F}_r = \boldsymbol{\Phi}_n^T\mathbf{F}$.

Finally, the discrete-time version of (8) that is used by the predictive controllers, was obtained using the bilinear transformation with a sampling time of 0.2 s,

$$\mathbf{a}(k + 1) = \tilde{\mathbf{A}}\mathbf{a}(k) + \tilde{\mathbf{B}}\mathbf{u}(k) + \tilde{\mathbf{F}}\mathbf{d}(k) \qquad (9)$$

$$\mathbf{x}_n(k) = \boldsymbol{\Phi}_n\mathbf{a}(k),$$

where $\tilde{\mathbf{A}}$, $\tilde{\mathbf{B}}$ and $\tilde{\mathbf{F}}$ are the matrices describing the new system. The sampling time was chosen by dividing the smallest time constant of the system (8) by 10.

IV. PREDICTIVE CONTROL SCHEME

The control goal is to reject the disturbances that affect the reactor, that is the changes in the temperature and concentration of the feed flow. In addition, the control system must satisfy the input constraints of the process and it should keep the temperature inside the reactor below 400 K.

In [2], a POD-based MPC control scheme is proposed for controlling the reactor. Nevertheless this control scheme does not incorporate the temperature constraint of the system in its formulation. In [3], an extension of such control system is presented that takes into account the temperature constraint of the reactor and incorporates a mechanism for handling infeasibilities. This extension is described along this section.
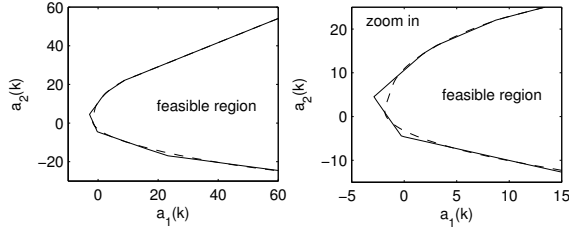
Fig. 3. Feasible region delimited by the temperature constraints of a 2nd order POD model. Dashed Line - Full set of constraints. Solid Line - 7 constraints chosen by the algorithm ($Sel = 0.08$ and $\gamma = 0.01\,(0.8\mathrm{K})$).
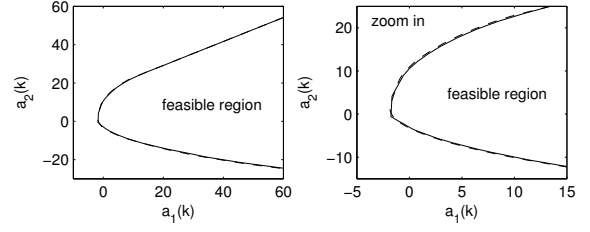

Fig. 4. Feasible region delimited by the temperature constraints of a 2nd order POD model. Dashed Line - Full set of constraints. Solid Line - 21 constraints chosen by the algorithm ($Sel = 0.022$ and $\gamma = 0.01\,(0.8\mathrm{K})$).

The control of the temperature and concentration profiles is achieved indirectly by controlling the POD coefficients. The references ($\mathbf{a}_{\mathrm{ref}}$) of these POD coefficients can be calculated by

$$\mathbf{a}_{\mathrm{ref}} = \mathbf{\Phi}_n^T \mathbf{x}_{\mathrm{ref}} \qquad (10)$$

where $\mathbf{x}_{\mathrm{ref}}$ is the reference of the vector $\mathbf{x}(t)$ and is equal to $\mathbf{0}$ since the control system has to keep the reactor operating around the profiles shown in Figure 2.

In order to handle the infeasibilities that can emerge, the MPC control scheme treats the temperature constraint as a soft constraint by using a *slack variable* approach with ℓ_∞-norm and time-dependent weights [4]. The MPC controller is formulated as follows:

$$\min_{a,\Delta u,\varepsilon} J = \sum_{k=1}^{N_{\mathrm{p}}} \|\mathbf{a}_{\mathrm{ref}} - \mathbf{a}(k)\|_{\mathbf{Q}}^2 + \sum_{k=0}^{N_{\mathrm{c}}-1} \|\Delta \mathbf{u}(k)\|_{\mathbf{R}}^2 + \quad (11a)$$

$$+ P_{\mathrm{Q}}\varepsilon^2 + P_{\mathrm{L}}\varepsilon$$

subject to

$$\mathbf{a}(k+1) = \tilde{\mathbf{A}}\mathbf{a}(k) + \tilde{\mathbf{B}}\mathbf{u}(k) + \tilde{\mathbf{F}}\mathbf{d}(k)$$

$$\mathbf{d}(k+1) = \mathbf{d}(k), \;\; \mathbf{u}_{\min} \le \mathbf{u}(k) \le \mathbf{u}_{\max}$$

$$\bar{\mathbf{T}}^{\Delta}(k) = \mathbf{\Phi}_{\mathrm{T}}\mathbf{a}(k) \le \bar{\mathbf{T}}^{\Delta\max} + \mathbf{1} \cdot \eta(k)\varepsilon \qquad (11b)$$

$$\varepsilon \ge 0 \qquad (11c)$$

where $\mathbf{Q}$ and $\mathbf{R}$ are weighting matrices ($\mathbf{Q} \succeq 0, \mathbf{R} \succeq 0$), $\|\mathbf{v}\|_{\mathbf{Q}}^2$ denotes $\mathbf{v}^T \mathbf{Q}\mathbf{v}$, N_{p} is the prediction horizon, N_{c} is the control horizon, $\mathbf{u}_{\min}$ and $\mathbf{u}_{\max}$ are the lower and upper bounds (hard constraints) of $\mathbf{u}(k)$, $\bar{\mathbf{T}}^{\Delta}(k) = \mathbf{\Phi}_{\mathrm{T}}\mathbf{a}(k)$ is a vector which contains the normalized deviations of the temperature profile, $\mathbf{\Phi}_{\mathrm{T}}$ is the lower part (the last $N = 300$ rows) of the matrix $\mathbf{\Phi}_n = \left(\mathbf{\Phi}_{\mathrm{C}}^T, \mathbf{\Phi}_{\mathrm{T}}^T\right)^T$ that is associated to the temperature profile, $\bar{\mathbf{T}}^{\Delta\max} = (400\mathrm{K} \cdot \mathbf{1} - \mathbf{T}^*)/T_{\mathrm{f}}$ is a vector that contains the maximal allowed temperature for each point of the reactor, ε is the slack variable (a scalar quantity), P_{Q} and P_{L} are weighting factors ($P_{\mathrm{Q}} > 0$, $P_{\mathrm{L}} > 0$), $\mathbf{1} \in \Re^{300}$ is a vector of 1's and $\eta(k) = 1/r^{k-1}$ is a time-dependent weight ($r > 1$).

Since the state vector $\mathbf{a}(k)$ is unknown and the changes in the concentration of the feed flow $d_1(k) = \bar{C}_{\mathrm{in}}^{\Delta}(k)$ are not measured directly, they are estimated by means of an observer with the following formulation:

$$\begin{pmatrix} \hat{\mathbf{a}}(k+1) \\ \hat{d}_1(k+1) \end{pmatrix} = \begin{pmatrix} \tilde{\mathbf{A}} & \tilde{\mathbf{F}}_{\mathrm{C}} \\ \mathbf{0} & 1 \end{pmatrix} \begin{pmatrix} \hat{\mathbf{a}}(k) \\ \hat{d}_1(k) \end{pmatrix} + \begin{pmatrix} \tilde{\mathbf{B}} \\ \mathbf{0} \end{pmatrix} \mathbf{u}(k)$$

$$+ \begin{pmatrix} \tilde{\mathbf{F}}_{\mathrm{T}} \\ 0 \end{pmatrix} d_2(k) + \begin{pmatrix} \mathbf{L}_{\mathrm{a}} \\ \mathbf{L}_{\mathrm{d}} \end{pmatrix} (\mathbf{y}(k) - \hat{\mathbf{y}}(k)) \qquad (12a)$$

$$\hat{\mathbf{y}}(k) = \mathbf{C}_{\mathrm{s}}\hat{\mathbf{x}}_n(k) = \mathbf{C}_{\mathrm{s}}\mathbf{\Phi}_n\hat{\mathbf{a}}(k) \qquad (12b)$$

where $\hat{\mathbf{a}}(k)$ is the estimated vector of the POD coefficients, $\hat{d}_1(k)$ is the estimation of $\bar{C}_{\mathrm{in}}^{\Delta}(k)$, $d_2(k)$ is the normalized temperature deviation of the feed flow $\bar{T}_{\mathrm{in}}^{\Delta}(k)$, $\mathbf{y}(k) \in \Re^4$ is a vector which contains the four temperature measurements (normalized deviations) along the reactor, $\hat{\mathbf{y}}(k)$ is the estimate of $\mathbf{y}(k)$, $\mathbf{L}_{\mathrm{a}}$ and $\mathbf{L}_{\mathrm{d}}$ are the submatrices of the observer gain, $\tilde{\mathbf{F}}_{\mathrm{C}}$ and $\tilde{\mathbf{F}}_{\mathrm{T}}$ are the column vectors of $\tilde{\mathbf{F}} = (\tilde{\mathbf{F}}_{\mathrm{C}}, \tilde{\mathbf{F}}_{\mathrm{T}})$ and $\mathbf{C}_{\mathrm{s}}$ is a selection matrix which selects the measured temperatures from the vector $\mathbf{x}_n(k)$.

The control horizon N_{c} was set to 10 samples and the prediction horizon N_{p} was selected according to the following criterion: "Prediction Horizon = Control Horizon + Largest Settling Time = 80 samples". $\mathbf{u}_{\min}$ and $\mathbf{u}_{\max}$ were selected according to the input constraints of the process and the operating temperatures of the jackets. The other parameters were selected as follows: $r = 1.2$, $P_{\mathrm{L}} = 10^4$, $P_{\mathrm{Q}} = 10^4$, $\mathbf{Q} = \mathbf{I}_{20\times20}$ and $\mathbf{R} = 110 \cdot \mathbf{I}_{3\times3}$.

The MPC controller has to deal with $N \times N_{\mathrm{p}} = 300\times80 = 24\,000$ temperature constraints, which demand a considerable amount of memory, and computing power. Although the POD technique has reduced the number of state variables of (2), it is clear that the number of temperature constraints is still very large. In the next section an algorithm for reducing the number of temperature constraints is described.

V. REDUCTION OF THE NUMBER OF TEMPERATURE CONSTRAINTS

It has been observed that the coefficients of consecutive temperature constraints are quite similar. This is a consequence of the fact that the most relevant columns of $\mathbf{\Phi}_{\mathrm{T}}$ (the part of the POD basis vectors that is associated to the temperature profile) are smooth. By taking into account these observations, we propose an algorithm for selecting a reduced set of constraints from the full set. The output of the algorithm would be a matrix $\mathbf{\Phi}_{\mathrm{R}} \in \Re^{s_{\mathrm{c}} \times n}$ and a vector $\mathbf{T}_{\mathrm{R}} \in \Re^{s_{\mathrm{c}}}$ which define the new set of temperature constraints,

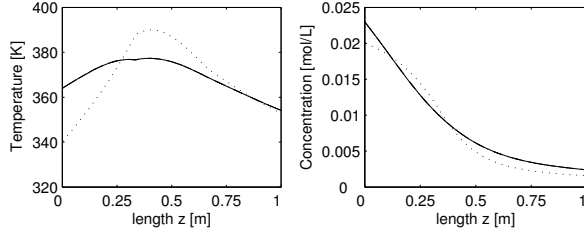$$\mathbf{\Phi}_{\mathrm{R}}\mathbf{a}(k) \le \mathbf{T}_{\mathrm{R}}. \qquad (13)$$

Fig. 5. Steady-State profiles after the test. Dotted line - reference. Solid Line - MPC-FC. Dashed line - MPC-RC. Dashdot line - MPC-NTC.

Fig. 6. Maximal peak of the temperature profile during the test. Solid Line - MPC-FC. Dashed line - MPC-RC. Dashdot line - MPC-NTC.

Here S_c is the number of selected constraints and n is the order of the POD model. In the description of the algorithm, the following notation is used: the ith row of the matrix $\mathbf{\Phi}_T$ and the ith entry of the vector $\bar{\mathbf{T}}^{\Delta_{\max}}$ are denoted by $\mathbf{\Phi}_T(i,:)$ and $\bar{\mathbf{T}}^{\Delta_{\max}}(i)$ respectively, the entry of the matrix $\mathbf{\Phi}_T$ that lies in the ith row and the jth column is written as $\mathbf{\Phi}_T(i,j)$, $\mathbf{\Phi}_R = [\mathbf{\Phi}_R; \mathbf{\Phi}_T(i,:)]$ indicates that ith row of $\mathbf{\Phi}_T$ is added at the bottom of the matrix $\mathbf{\Phi}_R$ and $\mathbf{T}_R = [\mathbf{T}_R; \bar{\mathbf{T}}^{\Delta_{\max}}(i)]$ denotes that the ith entry of the vector $\bar{\mathbf{T}}^{\Delta_{\max}}$ is added at the bottom of the vector $\mathbf{T}_R$. The proposed algorithm is the following one:

1) Set $p = 1$, and select the first constraint: $\mathbf{T}_R = \bar{\mathbf{T}}^{\Delta_{\max}}(1)$, $\mathbf{\Phi}_R = \mathbf{\Phi}_T(1,:)$.
2) For all $i = 2, \ldots, N - 1$, perform:
   a) Calculate the difference between the pth and ith constraints using this formula:

   $$d = \frac{1}{n+1}\left(\sum_{j=1}^{n}|\mathbf{\Phi}_T(p,j) - \mathbf{\Phi}_T(i,j)|+ \right.$$
   $$\left. + \left|\bar{\mathbf{T}}^{\Delta_{\max}}(p) - \bar{\mathbf{T}}^{\Delta_{\max}}(i)\right|\right)$$

   b) if $d \geq Sel$ then select the ith constraint:
      - $\mathbf{\Phi}_R = [\mathbf{\Phi}_R; \mathbf{\Phi}_T(i,:)]$.
      - if $(i-p) > 1$ then $\mathbf{T}_R = [\mathbf{T}_R; \bar{\mathbf{T}}^{\Delta_{\max}}(i) - \gamma]$ else $\mathbf{T}_R = [\mathbf{T}_R; \bar{\mathbf{T}}^{\Delta_{\max}}(i)]$.
      - Set $p = i$.
3) Select the last constraint: $\mathbf{T}_R = [\mathbf{T}_R; \bar{\mathbf{T}}^{\Delta_{\max}}(N)]$, $\mathbf{\Phi}_R = [\mathbf{\Phi}_T(1,:)]$.

where N is the number of sections in which the reactor is divided and therefore the number of temperature constraints, d is the mean absolute error between the coefficients of 2 constraints, Sel is the minimum value of d that is required for selecting a constraint, and γ is a parameter that is used to tighten non consecutive constraints $((i - p) > 1)$. The function of γ is to shrink a little bit the feasible region delimited by the reduced set of constraints, in such a way that by choosing an appropriated value of γ, no part of this feasible region is outside the region delimited by the full set of constraints. This is of course a conservative measure.

Although the POD model of the reactor has 20 states, in this section a 2nd order POD model is used in order to visualize the feasible regions delimited by the temperature constraints. Figures 3 and 4 show the feasible regions delimited by the constraints selected by the algorithm when
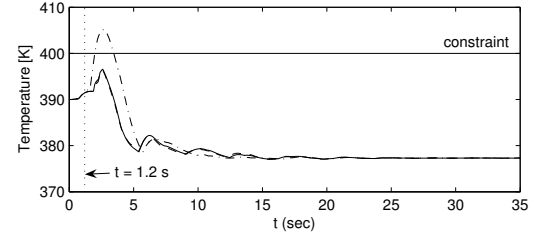
different values of Sel and γ were used. For $Sel = 0.08$ and $\gamma = 0.01 = 0.8\,\mathrm{K}/T_f$ $(T_f = 80\,\mathrm{K})$, the algorithm selected 7 constraints (see Figure 3) from 300. These 7 constraints provide a fair approximation of the feasible region of the original problem. For $Sel = 0.022$ and $\gamma = 0.01$ (0.8 K), the algorithm chose 21 constraints (see Figure 4). From Figure 4, it is remarkable how the feasible region delimited by 300 temperature constraints can be approximated accurately by only 21 constraints. It is important to remark that the algorithm does not guarantee that the selected set of constraints is the optimal one, in the sense that it minimizes the difference between the feasible regions delimited by the full and the reduced set of constraints.

The formulation of the new MPC controller based on a reduced set of temperature constraints would be given by (11), but substituting $\mathbf{\Phi}_T$ and $\bar{\mathbf{T}}^{\Delta_{\max}}$ by $\mathbf{\Phi}_R$ and $\mathbf{T}_R$ respectively in (11b), and by resizing properly the vector of 1's. This new MPC has the same tuning parameters as the MPC presented in Section V and it uses the same observer. We have set $Sel = 0.03$ and $\gamma = 0.00625$ (0.5 K) in the algorithm, and it has selected $S_c = 20$ constraints.

Unlike the MPC presented in Section V which deals with 24 000 temperature constraints, this MPC has only $S_c \times N_p = 20 \times 80 = 1600$ constraints. Hence, a large reduction in the number of temperature constraints has been achieved by means of the algorithm proposed in this paper. This reduction leads to a big saving of memory, since the reduced set of constraints (0.402 MB) require 14.7 times less memory than the complete set (5.91 MB).

VI. SIMULATION RESULTS

In order to perform the closed-loop simulations of the control systems described in the previous sections, the nonlinear model of the process given in (1) was discretized in space by replacing the partial derivatives with respect to space by backward difference approximations [5][8]. From now on, the MPC controller (11) will be referred to as MPC-FC and the MPC with a reduced set of temperature constraints to as MPC-RC.

Initially, in order to compare and evaluate the performance of the MPC controllers, we carried out the tests proposed in [2]. In these tests the temperature and the concentration of the feed flow are increased and decreased by 10 K and 10^{-3} mol/L respectively. The simulation results of MPC-FC and MPC-RC were quite similar to the ones shown in [2], where a POD-based MPC controller without temperature constraints is presented. The formulation of this controller is
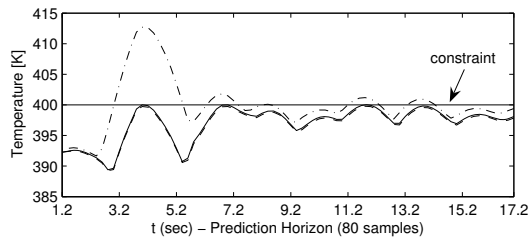
Fig. 7. Predictions of the maximal peak of the temperature profile at $t = 1.2$ s. Solid Line - MPC-FC. Dashed line - MPC-RC. Dashdot line - MPC-NTC.

given by (11) after eliminating the equations (11b), (11c) and the term $P_Q \varepsilon^2 + P_L \varepsilon$ in the cost function. This controller with No Temperature Constraints will be referred to as MPC-NTC. Along the tests, the MPC-FC, MPC-RC and MPC-NTC controllers kept the reactor working around the nominal operating profiles, there were no violations of the temperature constraint, the concentration in steady state at the reactor outlet was kept quite close to its nominal value, and the control actions were all the time within the allowed bounds.

The similarities in the results are because of the fact that the control systems were not operating close to the temperature constraints, and therefore during the tests, these constraints were not active in the MPC-FC and MPC-RC controllers. Therefore, in order to evaluate the ability of MPC-FC and MPC-RC to deal with the temperature constraints, we use the test proposed in [3]:

- Test: the temperature and concentration of the feed flow are increased by 24 K and $3 \cdot 10^{-3}$ mol/l respectively. These disturbances are large in comparison with the typical ones.

Notice that under this test, the tubular reactor operates far from the operating profiles shown in Figure 2, and therefore the differences between the nonlinear model of the process and the linear POD model used by the controllers are considerable. Figures 5 and 6 present the simulation results. From Figure 5 we can observe that for all the controllers, the steady state profiles of the reactor are overlapping. In Figure 6 we can see that for the case of the MPC-NTC controller, the temperature constraint is temporarily violated during 1.49 s with a maximal peak of 405.1 K. On the other hand, the MPC-FC and MPC-RC controllers keep the temperature profile below 400 K, and it is really hard to see any difference in their responses. Concerning the control actions of the MPC controllers, they were all the time within the allowed limits.

Figure 7 shows the controllers' predictions of the maximal peak of the temperature profile at $t = 1.2$ s. From Figure 7 it is clear that the temperature constraints of MPC-FC and MPC-RC are active. Both controllers keep the temperature below and on 400 K along the prediction horizon, and the difference between their predictions are practically negligible. Observe that in this test, the closed-loop response of the controlled system is different than the predicted one. This is mainly due to considerable differences between the linear POD model used by the controllers and the observer, and the

nonlinear model of the process.

The average times for solving the optimization problem (in a PC with a Pentium D of 3 Ghz and a RAM memory of 2 GB) were 0.53 s and 0.037 s for the MPC-FC and MPC-RC controllers respectively. The MPC-RC controller requires 14.32 times less time than the MPC-FC controller for solving the optimization. To sum up, the reduction in the number of temperature constraints by means of the algorithm proposed in this paper, has led to a big reduction in the computational time.

VII. CONCLUSIONS

In this paper, an algorithm for reducing the number of temperature constraints of a POD-based predictive controller for a tubular reactor has been presented. The algorithm leads to a significant reduction in the number of constraints, which conduces to a considerable saving of memory, and a substantial reduction in the computational time required for solving the optimization of the MPC controller. The predictive controller based on the reduced set of constraints presented a good behavior and it was able to deal with the temperature constraints quite well. Additionally, its behavior was practically identical to the behavior of the predictive controller based on the complete set of constraints.

VIII. ACKNOWLEDGMENTS

REFERENCES

[1] M. Hazenberg, P. Astrid, and S. Weiland, "Low order modeling and optimal control design of a heated plate," in *Proceedings of the 5th European Control Conference*, Cambridge, September 2003.

[2] O. M. Agudelo, J. J. Espinosa, and B. De Moor, "Control of a tubular chemical reactor by means of POD and predictive control techniques," in *Proceedings of the European Control Conference 2007 (ECC 2007)*, Kos, Greece, July 2007, pp. 1046–1053.

[3] O. M. Agudelo, M. Baes, J. J. Espinosa, B. De Moor, and M. Diehl, "Positive polynomial constraints for POD-based model predictive controllers," *Submitted to IEEE Transactions on Automatic Control, Special Issue on Positive Polynomials in Control*, 2007.

[4] M. Hovd and R. D. Braatz, "Handling state and output constraints in MPC using time-dependent weights," in *Proceedings of the American Control Conference (ACC)*, Arlington, USA, 2001.

[5] I. Y. Smets and J. F. Van Impe, "Optimal control of tubular chemical reactors: performance assessment under transient and diffuse conditions," in *Proceedings of the 10th Mediterranean Conference on Control and Automation - MED2002*, Lisbon, Portugal, 2002.

[6] M. Fjeld and B. Ursin, "Approximate lumped models of a tubular chemical reactor, and their use in feedback and feedforward control," in *Proceedings of the 2nd IFAC Symposium on Multivariable Technical Control Systems*, North Holland, Amsterdam, 1971, pp. 1–18.

[7] P. Astrid, "Reduction of process simulation models: a proper orthogonal decomposition approach," Ph.D. dissertation, Technishche Universiteit Eindhoven, Eindhoven (Netherlands), November 2004.

[8] D. Del Vecchio and N. Petit, "Boundary control for an industrial underactuated tubular chemical reactor," *Journal of Process Control*, vol. 15, pp. 771–784, 2005.